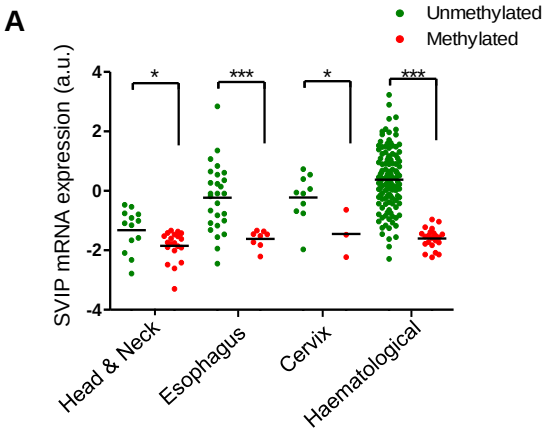

C

		Tissue	Cervix			Normal cervical tissue	Esophagus			Normal esophageal tissue
TargetID	**MAPINFO**	**Position**	Ca-Ski	HeLa	SW756		COLO-680N	KYSE-180	OACM 5.1C	
cg04255070	22851591	TSS1500	0.896	0.070	0.082	0.060	0.613	0.622	0.075	0.020
cg01593340	22851587	TSS1500	0.826	0.055	0.051	0.110	0.518	0.518	0.034	0.040
cg16113692	22851502	TSS200	0.964	0.073	0.072	0.030	0.625	0.785	0.018	0.010
cg26918510	22851422	TSS200	0.985	0.019	0.000	0.000	0.711	0.961	0.010	0.060
cg26821579	22851416	TSS200	0.988	0.083	0.058	0.000	0.387	0.955	0.021	0.050
cg01129966	22851401	TSS200	0.933	0.039	0.077	0.020	0.815	0.963	0.078	0.010
cg25421615	22851383	TSS200	0.958	0.033	0.006	0.000	0.447	0.971	0.037	0.020
cg17953636	22851321	1stExon	0.816	0.092	0.099	0.080	0.889	0.750	0.136	0.030

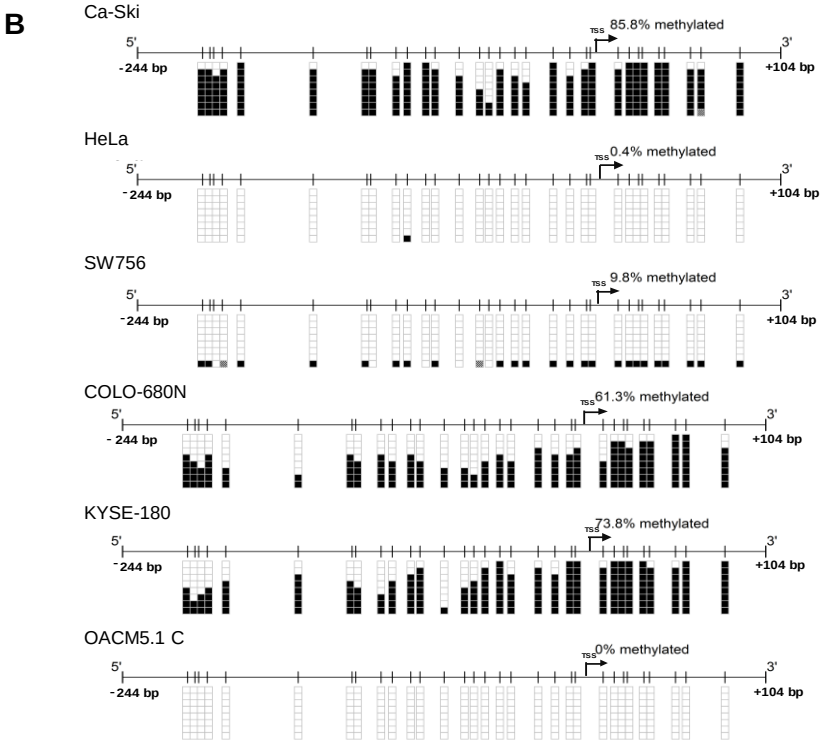

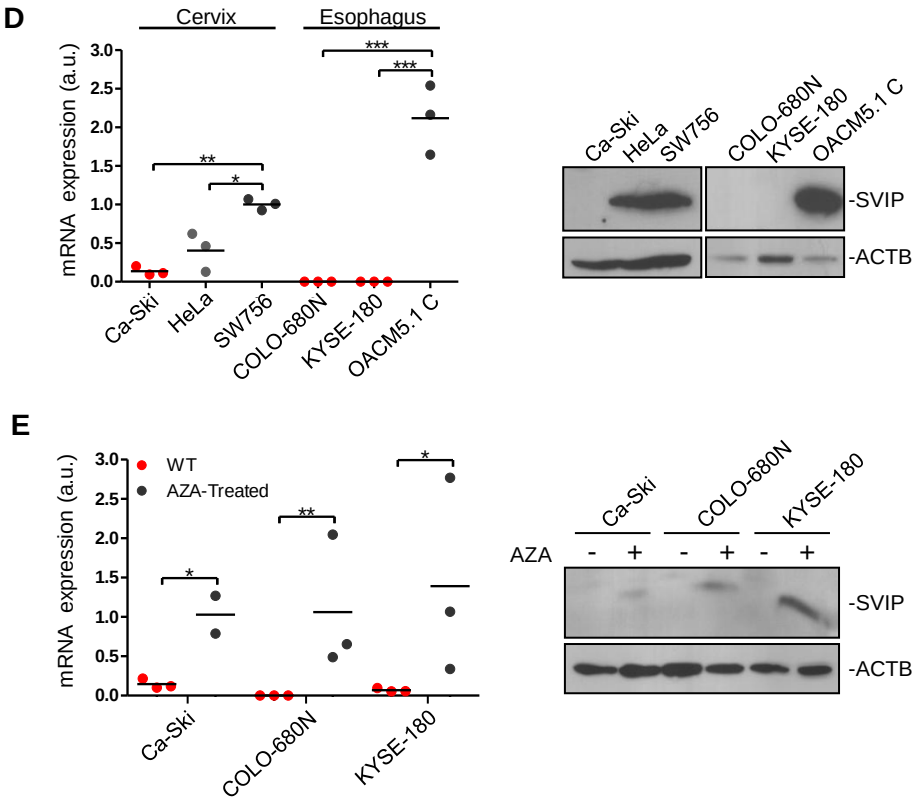

Supplemental Figure 1. Transcriptional silencing of *SVIP* by promoter CpG island hypermethylation in cervical and esophageal cancer cells. (**A**) SVIP expression analysis in head & neck, esophagus, cervix and haematological cell lines. A non-parametric Mann Whitney test was performed. (**B**) Bisulfite genomic sequencing of *SVIP* promoter CpG island in the studied cervical and esophageal cancer cells lines. CpG dinucleotides are represented as short vertical lines and the transcription start site (TSS) is represented as a long black arrow. Single clones are shown for each sample. Presence of an unmethylated or methylated cytosine is indicated by a white or black square, respectively. (**C**) DNA methylation profile of the CpG island promoter for the *SVIP* gene analyzed by the 450K DNA methylation microarray. Single CpG absolute methylation levels (0 – 1) are shown. Green, unmethylated; red, methylated. Data from three cervical (Ca-Ski, HeLa and SW756), three esophageal (COLO-680N, KYSE-180 and OACM 5.1C), normal cervical tissue and normal esophageal tissue are shown. (**D**) SVIP expression levels in cervical and esophageal cancer cell lines determined by real-time PCR (data shown represent mean.of biological replicates) (*left*) and western blot (*right*). (**E**) Expression of the SVIP RNA transcript (data shown represent the mean of biological replicates) (*left*) and protein (*right*) was restored in the SVIP epigenetically silent Ca-Ski, COLO-860N and KYSE-180 cells by treatment with the demethylating drug 5-aza-2'-deoxycytidine (AZA). qPCRs were analysed using a two tailed Student 's t-test. *P < 0.05, **P < 0.01, ***P < 0.001.

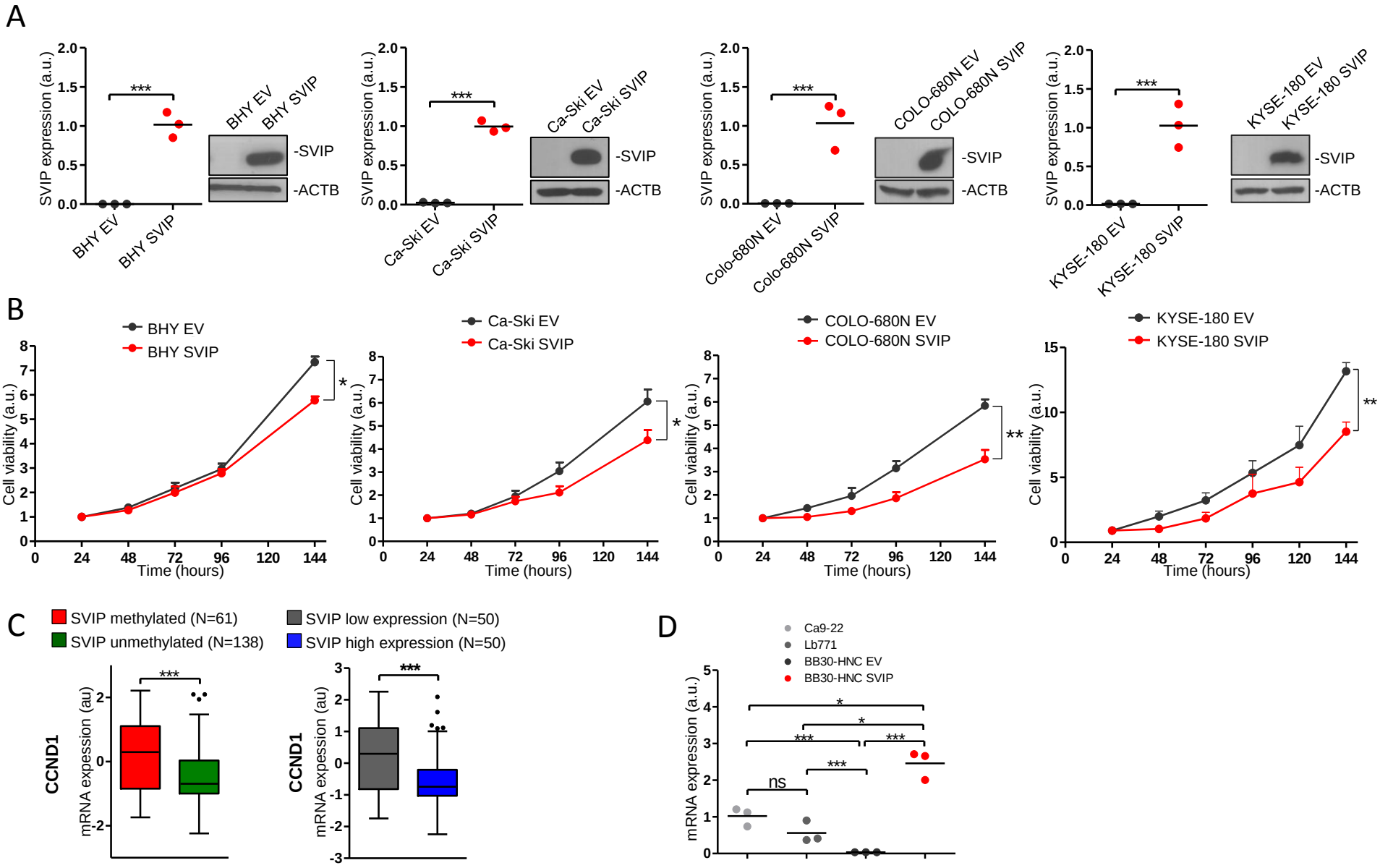

Supplemental Figure 2. Efficient restoration of SVIP in other cell lines. SVIP recovery upon transfection in BHY (head and neck cancer), Ca-Ski (cervical cancer), COLO-680N (esophageal cancer) and KYSE-180 (esophageal cancer) cancer cell lines was validated by (**A**) qRT-PCR (biological replicates are shown, statistical analysis was performed using a two-sided Student's t test) and western blot (images are representative of at least three different assays). (**B**) Cell viability was determined by SRB assay (graphs are representative of three independent experiments; statistical analysis was performed by comparing mean endpoints using two-tailed (**C**) In silico correlation of the expression of the cell cycle marker cyclin D1 depending on SVIP methylation and expression status in head and neck, esophageal, cervix and haematological cell lines. Samples whose SVIP expression was lower than the first quartile were considered "SVIP low", whereas samples with SVIP expression levels higher than the third quartile were considered "SVIP high". Two-tailed U-Mann Whitney test was performed to compare mRNA expression between the groups of cell lines and TCGA samples. (**D**) Comparison of the magnitude of SVIP overexpression in BB30-HNC cell line compared with two unmethylated cell lines, Ca9-22 and Lb771 by qPCR.*P < 0.05, **P < 0.01, ***P<0.001.

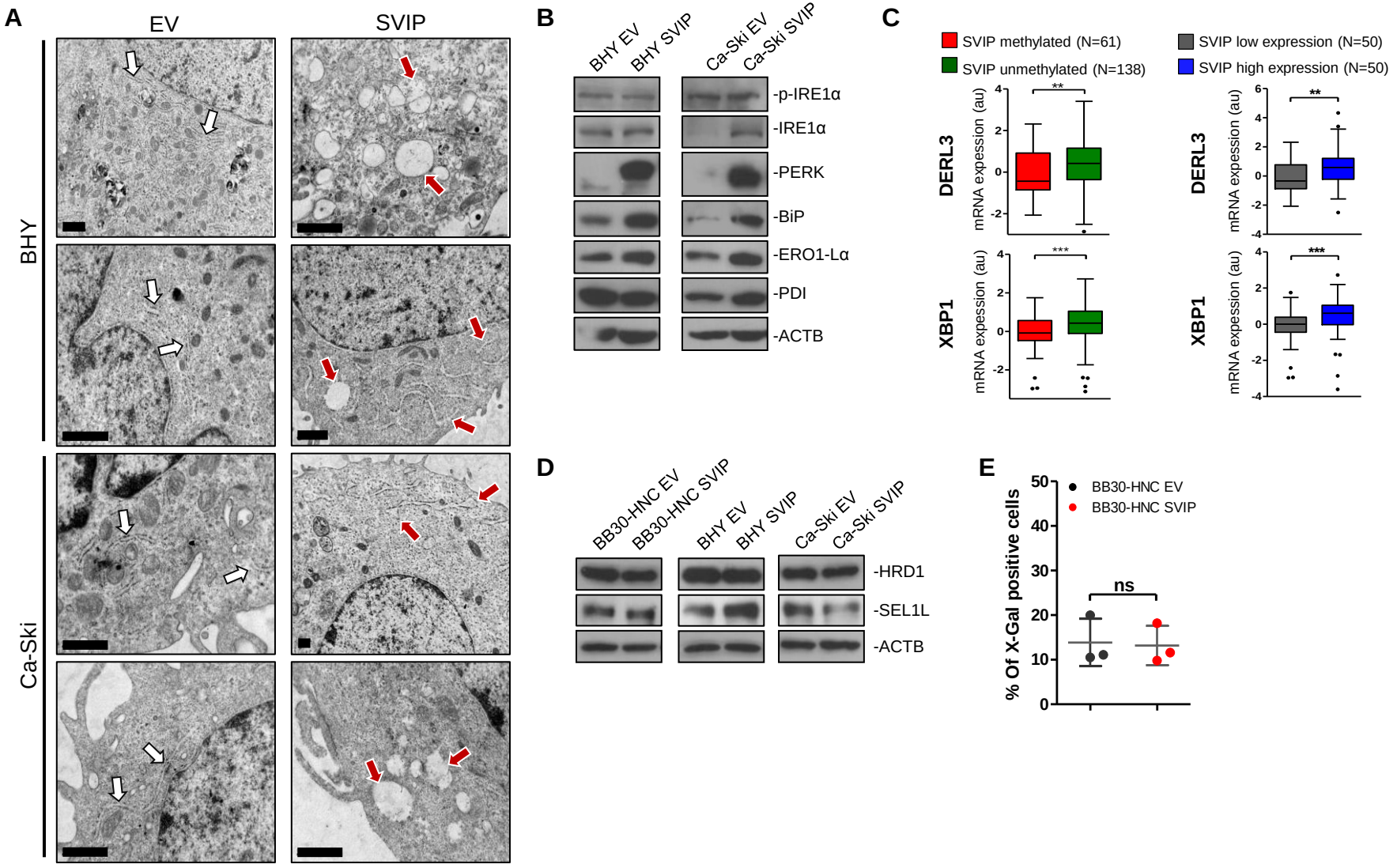

Supplemental Figure 3. Restoration of SVIP expression does not alter the expression of other proteins involved in ERAD machinery and also recapitulates the ER stress situation in BHY and Ca-Ski cell lines. (**A**) Electron microscopy images of empty vector-transfected and SVIP-expressing BHY and Ca-Ski cell lines. All scale bars represent 1µm. (**B**) Representative western blots of various proteins associated to UPR and protein folding in the ER after SVIP recovery in BHY and Ca-Ski cells. (**C**) In silico correlation of the expression of three ER-related proteins (AMFR, DERL3 and XBP1) depending on SVIP methylation and expression status in head and neck, esophageal, cervix and haematological cell lines and in head & neck TCGA cohort. Samples whose SVIP expression was lower than the first quartile were considered "SVIP low", whereas samples with SVIP expression levels higher than the third quartile were considered "SVIP high". Two-tailed U-Mann Whitney test was performed to compare mRNA expression between the groups of cell lines and TCGA samples. (**D**) Representative western blot of proteins involved in ERAD process after SVIP recovery in BB30-HNC, BHY and Ca-Ski cell lines. All western blots in B and D were performed in triplicate. (**E**) % of β-galactosidase-expressing cells in EV- and SVIP-transfected BB30-HNC cells. Statistical differences were determined using a two-sided Student's t test.

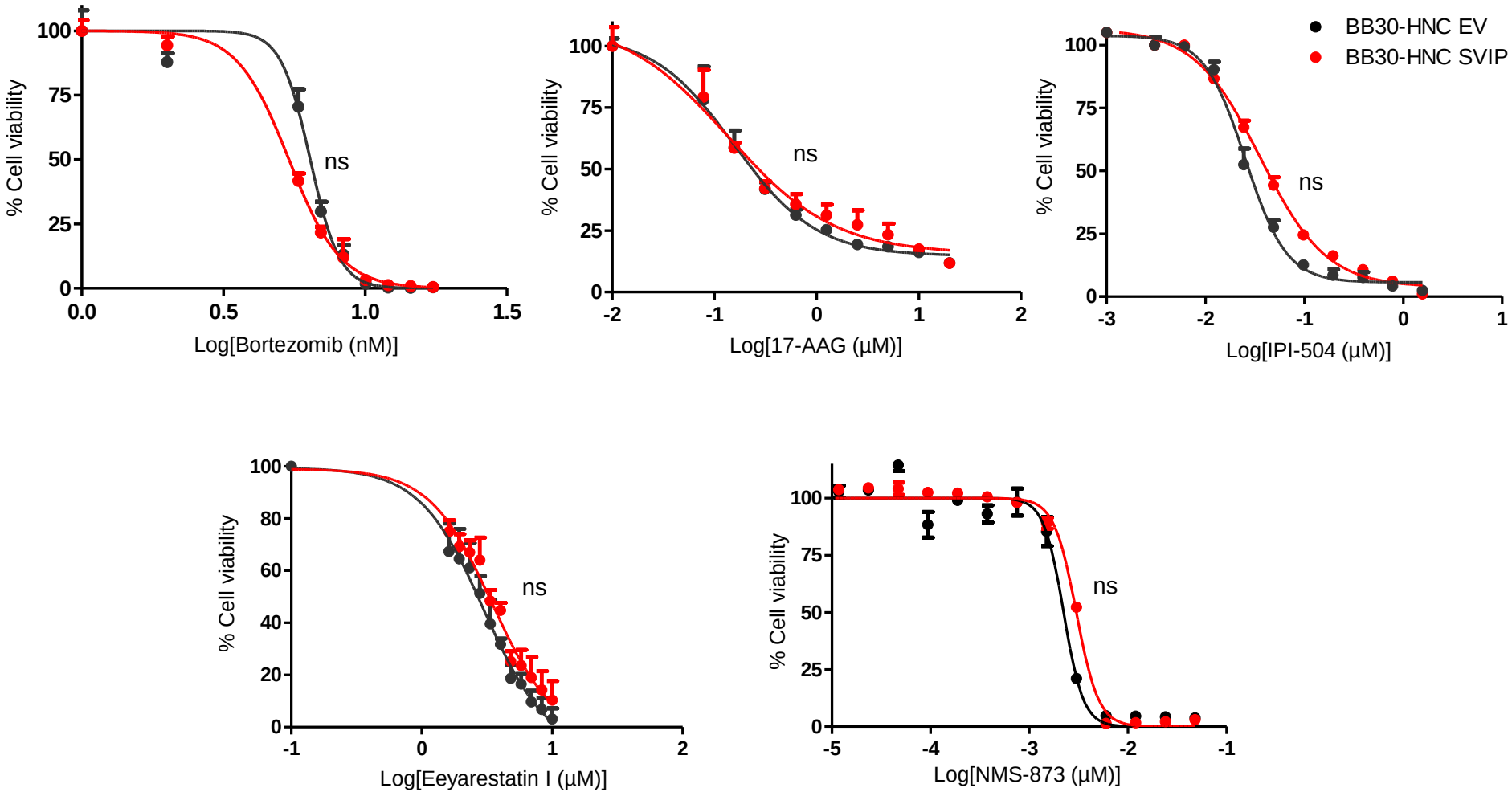

Supplemental Figure 4. ER-related drugs testing on BB30-HNC model. Determination of growth inhibitory effect by the SRB assay in empty vector and SVIP- transfected BB30-HNC cells upon treatemnet with Bortezomib, 17-AAG, IPI-504, Eeyarestatin I and NMS-873. All assays were performed in triplicate. Graphs are representative of the experiments. Statistical differences were determined by adjusting the curve to a third grade polynomic equation followed by extra sum of squares F-test. ns, no significant.

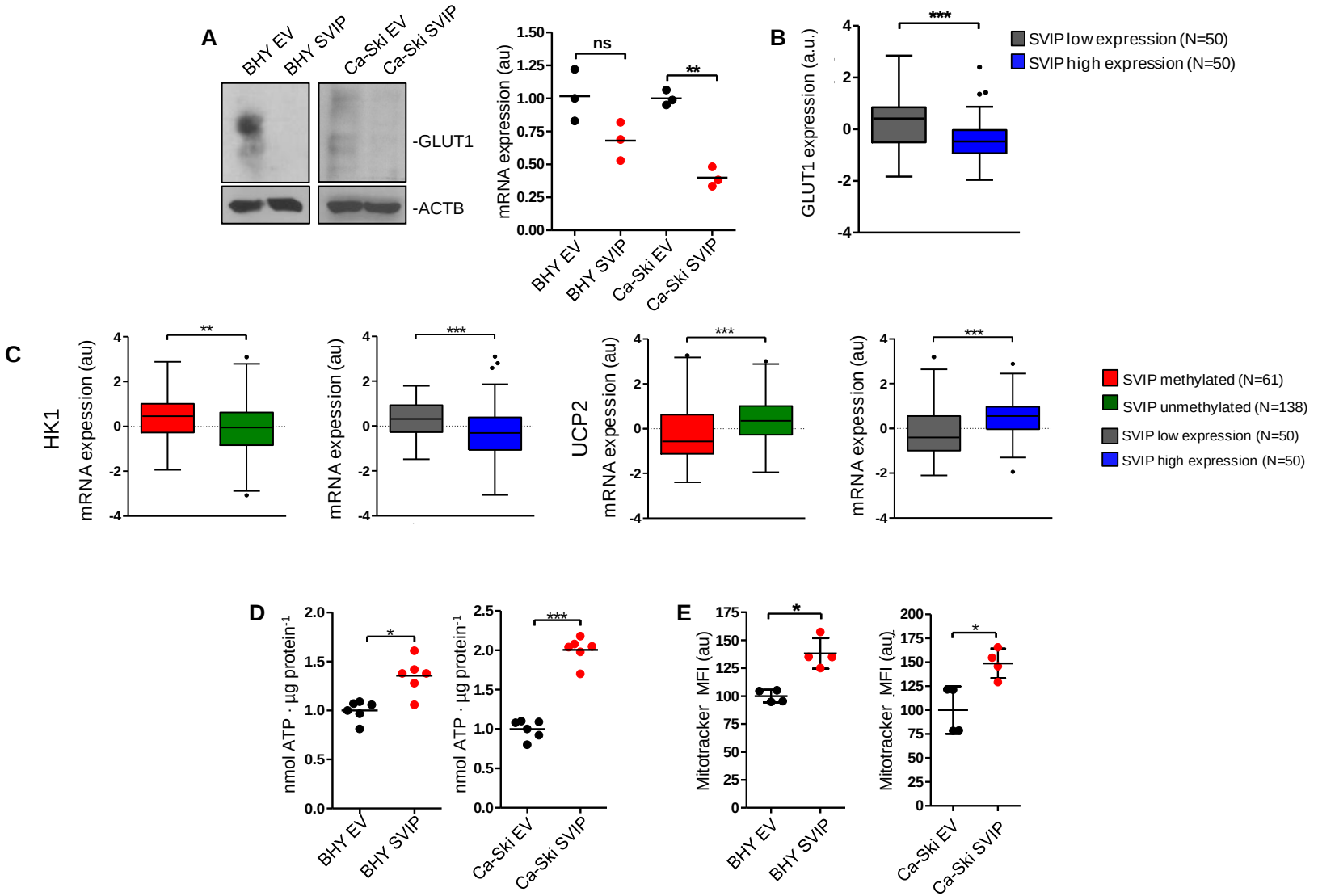

Supplemental Figure 5. Metabolic consequences of SVIP recovery in BHY and Ca-Ski cancer cell lines. (**A**) Western blot of GLUT1 in empty vector and SVIP-restored BHY and Ca-Ski cell lines. (**B**) SVIP mRNA expression significantly anticorrelates with GLUT1 mRNA expression in HNC, esophagus, cervix and haematological cell lines (N=118). SVIP expression was considered low when the when it was lower or equal than the first quartile, while SVIP expression was considered high when it was equal or higher than the third quartile. Expression was compared using a two-sided Mann-Whitney test. (**C**) In silico correlation of the expression of three metabolism-related proteins (HK1 and UCP2) depending on SVIP methylation and expression status in head and neck, esophageal, cervix and haematological cell lines and in head & neck TCGA cohort. Samples whose SVIP expression was lower than the first quartile were considered “SVIP low”, whereas samples with SVIP expression levels higher than the third quartile were considered “SVIP high”. Two-tailed U-Mann Whitney test was performed to compare mRNA expression between the groups of cell lines and TCGA samples. (**D**) ATP production in BHY and Ca-Ski cell lines upon SVIP transfection. Data were firstly normalized against protein amount, and then relativized against EV. Graph is representative of three independent experiments. Values are represented as mean of six replicates. Statistical differences have been reported using two-sided Student’s t-test. (**E**) Mito Tracker median fluorescence Intensity (MFI) was determined by flow cytometry. Mean SD of representative experiments is shown. (**G**). *P<0.05,**P<0.01,***P<0.001, ns no significant.

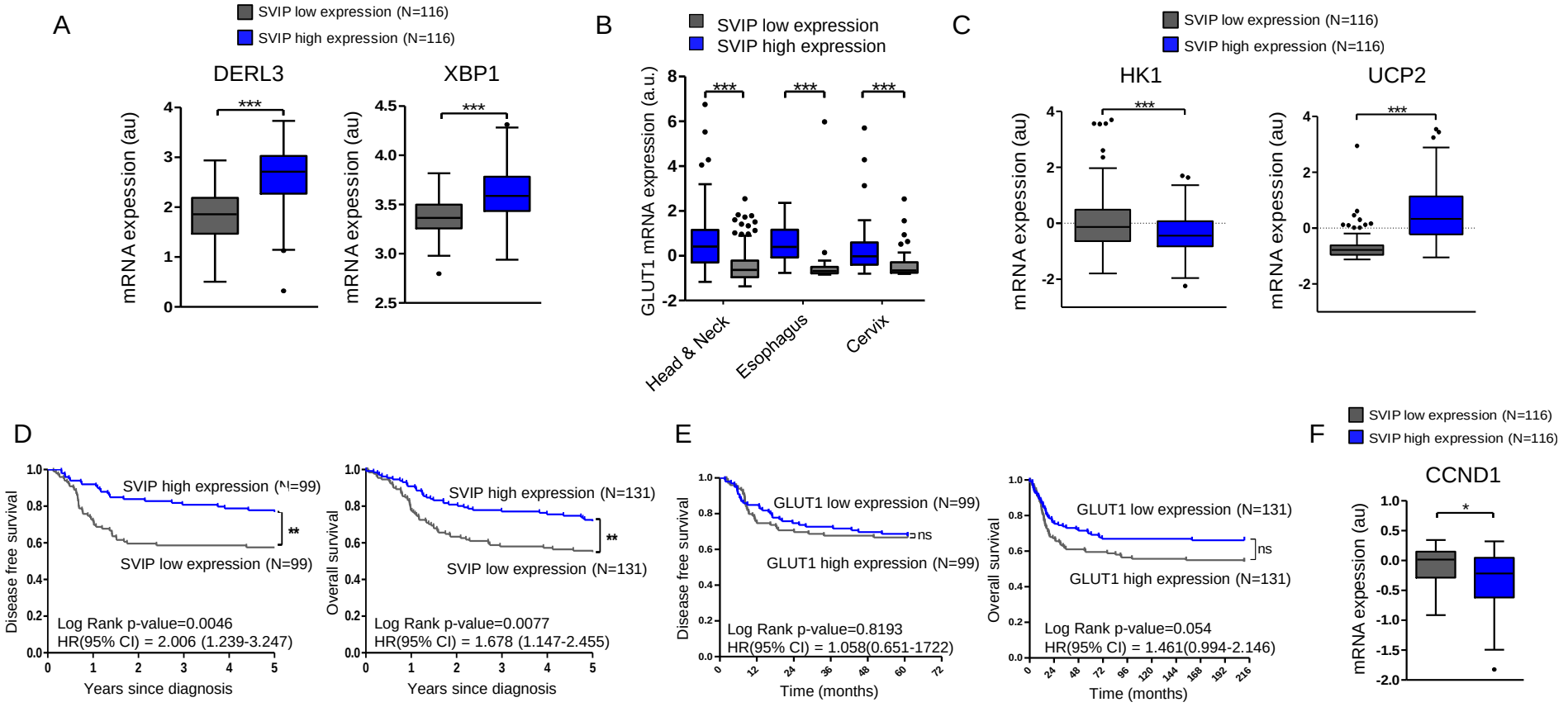

Supplemental figure 6. SVIP epigenetically-deficient head & neck TCGA tumors recapitulate the phenotype observed in SVIP-recovered cell lines. (**A**) In silico correlation of the expression of *XBP1* and *DERL3* depending on SVIP expression status in head & neck TCGA cohort. (**B**) GLUT1 expression analysis in head and neck, esophageal and cervical TCGA samples. (**B**) GLUT1 expression analysis in head and neck, esophageal and cervical TCGA samples depending on SVIP expression levels. (**C**) In silico correlation of the expression of *HK1* and *UCP2* depending on SVIP expression status in head & neck TCGA cohort. (**D**) Kaplan Meier analysis of disease free survival (left) and overall survival (right) considering SVIP expression in head and neck primary tumors of the TCGA data set. P- value corresponds to log rank test. Results of univariate Cox regression analysis are shown by hazard ratio (HR) and 95% confidence interval (CI). (**E**) Kaplan Meier analysis of disease free survival (left) and overall survival (right) considering GLUT1 expression in head and neck primary tumors of the TCGA data set. P- value corresponds to log rank test. Results of univariate Cox regression analysis are shown by hazard ratio (HR) and 95% confidence interval (CI). (**F**) In silico correlation of the expression of *CCND1* depending on SVIP expression status in head & neck TCGA cohort. Samples in all panels were divided in quartiles according to SVIP or GLUT1 expression. Samples whose SVIP/GLUT1 expression was lower than the first quartile were considered “low”, whereas samples with expression levels higher than the third quartile were considered “high. Two-tailed U-Mann Whitney test was performed to compare gene expression between the studied groups of cell lines and TCGA samples. *P<0.05,**P<0.01,***P<0.001, ns no significant.

Supplementary Table 1: List of differentially expressed proteins represented for at least two peptides in SILAC analysis upon SVIP transfection in BB30-HNC cells.

A. Upregulated upon SVIP overexpression

ID Gene	Fold change	p-value
FXR1	32.1428571	0.0299974
DHCR7	15.1020408	1.6286E-05
RTCA	12.8333333	0.04864284
VIM	10.617284	0.04760836
CNN3	10.1557632	0.02364341
HMGCS1	8.80090498	0.003165
LPCAT1	7.62942779	0.04977868
COPS8	7.34375	0.04210733
AP3S1	7.26744186	0.0199053
ABCD3	6.91333982	0.03893685
SLC25A24	6.82983683	0.04516253
CAT	5.85714286	0.00127963
PAIP1	5.55555556	0.0228933
VAT1	5.52857143	0.00319767
DNM2	5.37634409	0.04575119
IDH1	5.20661157	0.03582669
ITGA2	5.10416667	0.04200355
TARS	5.03846154	0.04664995
CTTN	4.95495495	0.02048994
ACAT2	4.60063898	0.00282376
RBM12	4.57142857	0.00441503
EIF2AK2	4.50980392	0.04177745
ERAP1	4.48514851	0.04793058
DCDC5	4.47368421	0.01507317
OSBP	4.44444444	0.01913367
S100A13	4.41176471	0.04020444
PPP2R2A	4.375	0.00362953
TKT	4.21232877	0.01032101
DDAH1	4.20588235	0.02980616
CYB5A	4.12612613	0.02691284
CUL4B	4.07619048	0.03584337
GDI1	3.93364929	0.02618891
PRKCDBP	3.92215569	0.01801815
PGM1	3.84615385	0.02005603
BASP1	3.70588235	0.00228101
SUB1	3.66666667	0.01454491
RRM2	3.6	0.00576178
G6PD	3.47692308	0.01762289
DTD1	3.4502924	0.03773559
MCTS1	3.4351145	0.0028799

ID Gene	Fold change	p-value
OGFR	3.42857143	0.04988295
PDIA6	3.41463415	0.01552488
KRT8	3.36585366	0.03671742
SUCLG2	3.34650856	0.01987182
GNAS	3.34117647	0.01566528
AKR1C1	3.32653061	0.04096684
RAB10	3.27058824	0.04417397
MTHFD1	3.25203252	0.01294349
RNPS1	3.24817518	0.03883771
ADIRF	3.22988506	0.01315107
GNB2	3.2183908	0.00195006
APEX1	3.2173913	0.01636789
NDUFB11	3.20512821	0.01195103
DENR	3.18181818	0.006425
PDPN	3.16363636	0.03425198
HADHB	3.08457711	0.04654997
UGDH	3.03478261	0.01298571
NUDT5	3.02325581	0.00117976
PSMF1	2.97752809	0.00378019
SLC25A5	2.96482412	0.01368587
MVP	2.92517007	0.03508987
GNAI2	2.92307692	0.00454258
APP	2.91727141	0.01900122
CORO1C	2.87096774	0.01134609
AKR1B1	2.85714286	0.03850582
LTA4H	2.84415584	0.03016842
PAFAH1B3	2.77966102	0.0310627
ACSL3	2.76960784	0.02925421
VCL	2.75630252	0.04905471
S100A6	2.7480916	0.00856122
SLC25A22	2.73737374	0.0198122
PGK1	2.72857143	0.04693298
CD82	2.72821577	0.0367791
MARS	2.7027027	0.0370125
HIBADH	2.68421053	0.00494985
MT-CO2	2.67409471	0.04651879
DDX1	2.62626263	0.03135003
ERP29	2.62365591	0.03317915
MAPRE1	2.59722222	0.00459747
APEH	2.5748503	0.00782955
AIFM1	2.57425743	0.02232868
KIF5B	2.5462963	0.02511471
NUMA1	2.5	0.02771502
PFKFB2	2.48863636	0.0479245
ECI1	2.47191011	0.01217441

ID Gene	Fold change	p-value
PREP	2.46808511	4.0259E-05
RALY	2.46153846	0.03930777
MBOAT7	2.45901639	0.039528
YBX3	2.42105263	0.02324571
PRDX5	2.4137931	0.00031503
GSTO1	2.36538462	0.04432432
CLNS1A	2.35443038	0.04334824
HADHA	2.32365145	0.00628803
SRI	2.31944444	0.01029654
ARHGAP1	2.31428571	0.00012989
TM9SF4	2.29885057	0.04998547
AARS	2.29032258	0.0073872
APMAP	2.28571429	0.00265961
RAB6C	2.25663717	0.04348661
ARPC2	2.24489796	0.03437383
RBBP4	2.17898833	0.04339225
TSPO	2.17333333	0.03546801
CLIC4	2.1541502	0.0188887
SARS	2.15	0.03363727
PRDX6	2.12765957	0.03805794
NUDT21	2.10918114	0.04786461
PKP1	2.09146341	0.03078166
RAVER1	2.06293706	0.04912038
CDC37	2.05555556	0.03594591
EIF1	2.05417607	0.02626985

B. Downregulated upon SVIP overexpression

ID Gene	Fold change	p-value
SIX5	0.02891892	0.02429929
TYMP	0.03857143	0.01735944
GSTP1	0.0401626	0.04078133
HSPB1	0.04258065	0.01581999
HLA-C	0.05031447	0.04112482
HLA-B	0.26961326	0.02763397
BICD2	0.27108434	0.00847096
ETFA	0.34016393	0.04288903
ETFB	0.35632184	0.00542287
APRT	0.36363636	0.04489244
ARPC5L	0.37623762	0.04469599
CLTB	0.38888889	0.04566731
PC	0.41958763	0.04420214
SLC2A1	0.46545455	0.0214964

Supplementary Table 2: Association between clinicopathological characteristics and SVIP methylation status in the TCGA head & neck squamous cell carcinoma cohort.

CHARACTERISTICS		SVIP methylation status		
	N (%)	Unmethylated N (%)	Methylated N (%)	P*
Age (years)				
< 50	48 (17%)	32 (67%)	16 (33%)	0.264
> 50	234 (83%)	135 (58%)	99 (42%)	
Gender				
Male	200 (71%)	130 (65%)	70 (35%)	0.003**
Female	82 (29%)	37 (45%)	45 (55%)	
Disease stage at diagnosis				
I	11 (4%)	7 (64%)	4 (36%)	0.207
II	55 (19%)	27 (49%)	28 (51%)	
III	67 (24%)	37 (55%)	30 (45%)	
IV	136 (48%)	88 (65%)	48 (35%)	
Unknown	13 (5%)	8 (62%)	5 (38%)	
Tumor site				
Oral cavity	104 (37%)	41 (39%)	63 (61%)	<0.001***
Tongue	92 (33%)	55 (60%)	37 (40%)	
Tonsil	16 (6%)	15 (94%)	1 (6%)	
Pharynx	10 (4%)	9 (90%)	1 (10%)	
Larynx	59 (21%)	47 (80%)	12 (20%)	
Unknown	1 (1%)	0 (0%)	1 (100%)	
Smoking habit				
Current / Former smoker	15 (5%)	7 (47%)	8 (53%)	0.287
Never smoker	185 (66%)	109 (59%)	76 (41%)	
Unknown	82 (29%)	51 (62%)	31 (38%)	
Drinking habits				
Yes	177 (63%)	114 (64%)	63 (36%)	0.031*
No	100 (35%)	51 (51%)	49 (49%)	
Unknown	5 (2%)	2 (40%)	3 (60%)	
HPV status				
Negative	49 (17%)	37 (75%)	12 (25%)	0.358
Positive	23 (8%)	20 (87%)	3 (13%)	
Unknown	210 (75%)	110 (52%)	100 (48%)	
Treatment strategy				
Surgery	94 (34%)	55 (58%)	39 (42%)	0.096
Chemotherapy	40 (14%)	31 (12%)	9 (23%)	
Radiotherapy	32 (11%)	22 (69%)	10 (31%)	
Unknown	116 (41%)	59 (51%)	57 (49%)	
Treatment outcome				
Complete remission/Response	171 (61%)	108 (63%)	63 (37%)	0.650
Stable disease	7 (2%)	5 (71%)	2 (29%)	
Progressive disease	44 (16%)	25 (57%)	19 (43%)	
Unknown	60 (21%)	29 (48%)	31 (52%)	
Survival status				
Alive	200 (71%)	127 (63%)	73 (37%)	0.024*
Dead	82 (29%)	40 (49%)	42 (51%)	

P-value represents Fisher's exact test or Chi-square function whenever required: statistical significance under 0.05, 0.01** and 0.001***

KEY RESOURCES TABLE

REAGENT or RESOURCE	SOURCE	IDENTIFIER
Antibodies		
SVIP	SIGMA	HPA039807
phospho-IRE1α (Ser724)	Thermofisher	PA1-16927
p21	CST	2947
eIF2α	CST	5324
phospho-eIF2α (Ser51)	CST	3398
SEL1L	Abcam	Ab78298
SYVN1 (Hrd1)	CST	14773
IRE1α	CST	14C10
PERK	CST	D11A8
ERO1-Lα	CST	#3264
PDI	CST	C81H6
BECLIN1	CST	D40C5
p62/SQTM	CST	#5114
LC3BI/II	CST	D3U4C
PARP	BD Pharmingen	556362
Caspase 3	SCBT	H-277
HM13	Abcam	ab190253
REEP5	SIGMA	HPA003895
CD82	Abcam	ab66400
NSDHL	Abcam	ab190353
SLC25A5	CST	#14671
SUCLG2	Abcam	ab96172
NDUFB8 (CI)	Abcam	ab110411
MTCO2 (CIV)	Abcam	ab110411
SLC2A1	CST	D3J3A
αTubulin-HRP	Abcam	40742
LMNB1	Abcam	ab16048
ACTB -HRP	SIGMA	A3854
Anti-rabbit HRP	SIGMA	A0545
Anti-mouse HRP	GE HEALTHCARE	NA9310
Bacterial and Virus Strains		
E. coli DH5α	Thermofisher	18265017
Lentivirus produced with PsPPAX and PDM2 plasmids	-	-
Chemicals, Peptides, and Recombinant Proteins		
5'-azacytidine	SIGMA	A2385
Sulforhodamine B	SIGMA	S1402
Polyethylene glycol 300	SIGMA	90878-1L
NMP	SIGMA	494496-1L
GoScript	Promega	A5001
Sybr green	Thermofisher	4312704
jetPrime polyplus	Polyplus	Ref114
Bortezomib	LC laboratories	B-1408
Eeyarestatin I	SIGMA	E1286
17-AAG	SIGMA	A8476
IPI-504	Medchem	HY-10210
Thapsigargin	SIGMA	T9033
SILAC-Lys8-Arg10-Kit media	SILANTES	282986444
Bay-876	Sigma	SML1774
NMS-873	MedChemExpress	HY-15713

Oligomycin	SIGMA	75351
FCCP	SIGMA	C2920
Rotenone A	SIGMA	R8875
Antimycin A	SIGMA	A8674
Hydrazine	Sigma	53847
NAD+	Roche - Sigma	10127990001
LDH	Roche - Sigma	10107085001
dATP	NEBiolabs	N0440S
Mito Tracker	Thermofisher	M22426
MitoSox	Thermofisher	M36008
U-$^{13}C_6$ labeled glucose	Sigma	389374
Critical Commercial Assays		
EZ-DNA methylation Gold Kit	Zimo research	D5006
Nucleospin Gel and PCR Clean-up	Machery Nagel	740609.250
Nucleospin 96 plasmid	Machery Nagel	740625.24
Maxwell RSC simply RNA tissue	Promega	AS1340
Seahorse XF24 plates	Agilent	100777-004
DC protein assay	BioRad	5000116
Cell titer Glo	Promega	G7571
Glucose HK CP	ABX diagnostics	A11A01667
Experimental Models: Cell Lines		
BB30-HNC	Sanger	CVCL_1076
BHY	DSMZ	CVCL_1086
Ca9-22	Sanger	CVCL_1102
LB-771	Sanger	CVCL_1369
Ca-Ski	ATCC	CVCL_1100
HeLa	ATCC	CVCL_0030
SW756	ATCC	CVCL_1727
COLO-680N	DSMZ	CVCL_1131
KYSE-180	DSMZ	CVCL_1349
OACM 5.1 C	SIGMA	11012006
HEK-293T	ATCC	CVCL_0063
Experimental Models: Organisms/Strains		
NU/NU Nude Mice	INVIGO	
Oligonucleotides		
BS SVIP F TTTTTTGGAATTTAGGTTTTGG	This paper	
BS SVIP R AAAAACACAACCCCATAAAAC	This paper	
Cloning SVIP S AAAAAAAAGAATTCGCCGCCACCATGGGGCTGTGTT TTCCTTGTCCCGGGGAGTCCGCGCCTC	This paper	
Cloning SVIP AS AAAAAAAAGGATCCTTACTTATCGTCGTCATCCTTGT AATCGCCGGAGCCTGAAACTGTCCACCTAAGTCCA CCTTCTGGTGGGGGCCCGGATGTAGCAA	This paper	
sh1_SVIP S gatccGACTTAGGTGGACAGTTTCTTCAAGAGAGAAA CTGTCCACCTAAGTCTTTTTTACGCGTg	This paper	
sh1_SVIP AS aattcACGCGTAAAAAAGACTTAGGTGGACAGTTTCTC TCTTGAAGAAACTGTCCACCTAAGTCg	This paper	
sh4_SVIP S gatccGGCTAGACTTTTCATTAAATTCAAGAGATTTAA TGAAAAGTCTAGCCTTTTTTACGCGTg	This paper	

sh4_SVIP AS aattcACGCGTAAAAAAGGCTAGACTTTTCATTAAATC TCTTGAATTTAATGAAAAGTCTAGCCg	This paper	
Scr_SVIP S gatccGCGCAGAACAAATTCGTCCATTCAAGAGATGG ACGAATTTGTTCTGCGTTTTTTACGCGTg	PMID: 28881673	
Scr_SVIP AS aattcACGCGTAAAAAACGCAGAACAAATTCGTCCATC TCTTGAATGGACGAATTTGTTCTGCGCg	PMID: 28881673	
q SVIP F AAAGAGCAAAGCTTGCAGAG	This paper	
q SVIP R GAAACTGTCCACCTAAGTCCAC	This paper	
q GAPDH F TGCACCACCAACTGCTTAGC	This paper	
q GAPDH R GGCATGGACTGTGGTCATGAG	This paper	
qSLC25A5 F CTACAAATCTGATGGATTAAGGG	This paper	
qSLC25A5 R ATGATGTCAGTTCCTTTGCG	This paper	
qSUCLG2 F CTGATCCTAAGGTTGAAGCCA	This paper	
qSUCLG2 R CGCTGTTGTTGAGTATCTTCTG	This paper	
qNDUFB8 F CCCTATCCTAGGACCCCAGA	This paper	
qNDUFB8 R TCCACACGGTTCCTGTTGTA	This paper	
qMT-CO2 F TTCATGATCACGCCCTCATA	This paper	
qMT-CO2 R TAAAGGATGCGTAGGGATGG	This paper	
qHM13 F CAGACATGCCTGAAACAATCA	This paper	
qHM13 R GATTCCCAGCACGAAGAAAT	This paper	
qREEP5 F CTTCATCGCTCTTGGTGTCA	This paper	
qREEP5 R GGTCAGCCACTGGGTATCAT	This paper	
qCD82 F TGAGGACTGGCCTGTGTACC	This paper	
qCD82 R TTGGGACCTTGCTGTAGTC	This paper	
qNSDHL F GACCTTCCCTATGCCATGAA	This paper	
qNSDHL R CCAAGTTCTTCCCATTTCCA	This paper	
qSLC2A1 F CATCAACGCTGTCTTCTATTACTC	This paper	
qSLC2A1 R ATGCTCAGATAGGACATCCA	This paper	
Recombinant DNA		
PsPax2	Addgene	12260
PDM2.G	Addgene	12259
pLVX-Ires-ZSgreen1	Clonetech	632187
pLVX-shRNA2	Clonetech	632179
Software and Algorithms		
cgds-R package	The R project	
Bioedit	Bio-Soft	
SPSS	IBM	
GraphPad Prism 5	GraphPad Software, Inc	
Methyl Primer Express v1.0	Applied Biosystems	
Primer3	Source Forge	
UCSC genome browser	UCSC	